铬掺杂的锂离子电池正极材料 $LiVPO_4F$ 的制备以及电化学行为的研究

李宇展 周 震 任俊霞 高学平 阎 杰*
(南开大学新能源材料化学研究所,天津 300071)

摘要: 采用高温固相法 2 步合成了掺 Cr 的锂离子电池正极材料 $LiV_{1-x}Cr_xPO_4F$(x=0,0.01,0.03,0.05,0.07),XRD 测试表明 $LiV_{1-x}Cr_xPO_4F$ 属三斜晶系。通过恒电流充放电,循环伏安和交流阻抗实验表明:掺 Cr 后 $LiVPO_4F$ 正极材料更有利于锂离子的嵌入和嵌出,材料的放电容量和循环性能进一步提高,例如,铬掺杂的 $LiVPO_4F$ 样品在室温、0.2 C 倍率下充放电,循环 50 周后容量在 110 mAh·g^{-1} 以上。文中还讨论了充放电容量随掺 Cr 量的关系,n_{Cr} 含量为 0.03 的 $LiV_{1-x}Cr_xPO_4F$ 有着较高的放电平台和良好的循环稳定性。

关键词: 锂离子电池;$LiVPO_4F$; 铬掺杂;循环伏安(CV)
中图分类号: O613.41; O614.51$^+$ **文献表示码**: A **文章编号**: 1001-4861(2006)03-0477-06

Preparation of Cr-doped $LiVPO_4F$ and Electrochemical Studies on Li Extraction/Insertion Performances for Lithium-ion Batteries

LI Yu-Zhan ZHOU Zhen REN Jun-Xia GAO Xue-Ping YAN Jie*
(*Institute of New Energy Material Chemistry, Nankai University, Tianjin* 30007)

Abstract: A series of Cr-doped $LiVPO_4F$ cathode materials were synthesized by conventional solid-state reactions of the stoichiometric mixture of VPO_4, $CrPO_4$ and LiF, and the samples showed the same triclinic structure as the undoped $LiVPO_4F$. The Cr-doped $LiVPO_4F$ samples were investigated on the Li extraction/insertion performances through galvanostatic charge/discharge, cyclic voltammetry (CV), and electrochemical impedance spectrum (EIS). The Cr-doped $LiVPO_4F$ systems showed improved capacity and cyclability in the voltage range of 3.0~4.6 V at different rates, for example, the measured discharge capacity of the Cr-doped $LiVPO_4F$ sample was still held over 110 mAh·g^{-1} after 50 cycles at 0.2 C rate at room temperature. The optimal doping content of Cr was that x=0.03 in the $LiV_{1-x}Cr_xPO_4F$ samples to achieve high discharge capacity and good cyclic stability. The electrode reaction reversibility was enhanced, and the charge transfer resistance was decreased through the Cr-doping. The improved electrochemical performances of the Cr-doped $LiVPO_4F$ cathode materials are attributed to the structural stability derived from the incorporation of Cr^{3+} ions.

Key words: lithium-ion batteries; $LiVPO_4F$; Cr-doping; cyclic voltammetry (CV)

0 Introduction

Since the birth in the early 1990′s, lithium ion batteries have been widely used in portable devices such as cellular phones, notebook-type computers etc. due to high energy density, good cyclic performance and excellent capacity retention. However, the ever-growing demand for lithium ion batteries has been

收稿日期:2005-10-17。收修改稿日期:2005-12-28。
国家重点基础研究发展规划资助项目(No.2002CB211800)。
*通讯联系人。E-mail:yanjie@nankai.edu.cn
第一作者:李宇展,女,33 岁,博士研究生;研究方向:无机材料与合成。

spawning more and more explorations of novel lithium insertion materials both for cathodes and anodes[1-4]. In lithium-ion rechargeable batteries, $LiCoO_2$ and spinel $LiMn_2O_4$ are currently used as cathode materials, but alternative cathode materials have been pursued to replace them. A good cathode material should have large capacity that can be retained for up to 1 000 cycles, good stability that can withstand fast recharge and discharge and some other possible extreme conditions, high affordablility for consumer electronics and large scale storage, and low toxicity.

In recent years, novel compounds based on transition metal polyanions have been proposed as a new class of cathode materials for lithium ion batteries[5-8]. At present there is great interest in synthesizing new phosphate or fluorophosphates with open structures because of their potential applications[9]. Certain lithium fluorophosphates turn out to be fascinating from a crystal-chemical point of view because of the particular behavior of the Li^+ ion in the presence of PO_4^{3-} group. The Li extraction/insertion properties of $LiVPO_4F$ were intensively studied in Barker′s group[10-12]. $LiVPO_4F$ is isostructural with the naturally occurring mineral tavorite, $LiFePO_4 \cdot OH$, crystallized with a triclinic structure (space group $P\bar{1}$). The reversible Li extraction/insertion reaction for $Li_{1-x}VPO_4F$, based on the V^{3+}/V^{4+} redox couple operates at about 4.2 V vs Li^+/Li[11,12]. However, the capacity of $LiVPO_4F$ decreases quickly during charge/discharge cycles, probably due to the phase instability, so before the practical application, long-term cyclic ability must be improved. We have recently found that the B-doping could improve the cyclic ability of $LiVPO_4F$ cathode material. In this work, Cr-doped $LiVPO_4F$ cathode material was synthesized, and the Cr-doping effect was investigated on the electrochemical performances of the $LiVPO_4F$ cathode material. The Cr-doping was also found to increase the discharge capacity and enhance the cyclic ability of $LiVPO_4F$ cathode material.

1 Experimental

1.1 Synthesis of $LiV_{1-x}Cr_xPO_4F$ ($0.00 \leqslant x \leqslant 0.07$)

Undoped and Cr-doped $LiVPO_4F$ cathode materials were synthesized by solid state reaction at high temperature. Firstly, a stoichiometric mixture of V_2O_5, $NH_4H_2PO_4$ and carbon was thoroughly mixed, and then pressed into pellets and heated at 300 ℃ in a tube furnace with a flowing argon gas for 4 h. After slowly cooled down to room temperature, the pellets were ground for 20 min, pressed into pellets again, heated to 750 ℃, and held at this temperature for 6 h. The pellets were cooled to room temperature, and ground into fine VPO_4 powder for further use. Similarly, $CrPO_4$ was synthesized at 900 ℃ for 8 h in air. Secondly, a stoichiometric mixture of VPO_4, $CrPO_4$ and LiF was thoroughly mixed, pressed into pellets, and sintered at 750 ℃ for 15 min in a tube furnace with a flowing argon gas. Finally, the $LiV_{1-x}Cr_xPO_4F$ product was cooled to room temperature rapidly and ground into fine powder. The undoped $LiVPO_4F$ sample was also prepared for comparison through the same procedure except the addition of $CrPO_4$.

1.2 Material characterization

Undoped and Cr-doped $LiVPO_4F$ were characterized with 2θ between 3° to 50° by X-ray diffraction (XRD) using a D/Max Ⅲ diffractometer with Cu $K\alpha$ radiation, at the scan rate of $8° \cdot min^{-1}$, and voltage of the 40 kV, current of 100 mA.

1.3 Electrochemical tests

Teflon-type test cells were assembled for all the electrochemical tests with undoped and Cr-doped $LiVPO_4F$ samples as active materials in the cathodes, respectively. A mixture of 77wt% active materials, 18wt% carbon black and 5wt% colloidal polytetrafluoroethylene (PTFE) binder was pressed into a circular pellet electrode with a diameter of 8 mm. The pellet was then dried at 100 ℃ for 24 h. The test cells were assembled with the above electrode as cathode and Li metal as anode in a dry glove box filled with argon gas. The electrolyte was 1 $mol \cdot L^{-1}$ $LiPF_6$ dissolved in a mixture of ethylene carbonate (EC) and dimethyl carbonate (DMC) with the volume ratio of 1∶1.

Charge/discharge cycling tests were performed using a commercial battery tester. The test cells were galvanostatically charged and discharged in the voltage range of 3.0~4.6 V. Cyclic voltammogram (CV)

was measured at a scan rate of 0.1 $mV \cdot s^{-1}$ using CHI 600A electrochemical analyzer. Electrochemical impendence spectrum (EIS) measurements were performed using a Solartron 1260 frequency response analyzer combined with a PAR 283 potentiostat. EIS measurements covered the frequency range of 10 kHz to 10 mHz with an ac voltage of 5 mV. The CV and EIS experiments were performed in the three-electrode system using metallic foils as both counter and reference electrode.

2 Results and discussion

2.1 XRD results

The XRD patters of $LiV_{1-x}Cr_xPO_4F$ (x=0.01, 0.03, 0.05, 0.07) are shown in Fig.1, and all the XRD patterns are similar to that of undoped $LiVPO_4F$. The diffraction peaks of all the samples are attributed to a pure single phase indexed with triclinic structure, and no other phases were detected in XRD analyses, indicating that Cr was doped completely into the crystal lattice of $LiVPO_4F$. Since the radius of V^{3+} is 0.074 nm, and the radius of Cr^{3+} is 0.064 nm. The Cr^{3+} ions may be mostly located at the position of V^{3+} in the crystal lattice. Accordingly, the Cr doping does not change the basic $LiVPO_4F$ crystal structure.

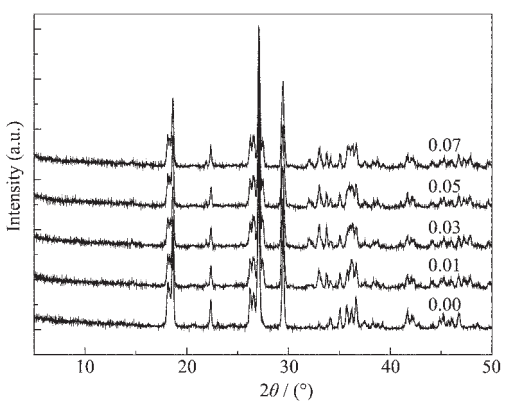

Fig.1 XRD patters for undoped and Cr-doped $LiVPO_4F$ ($LiV_{1-x}Cr_xPO_4F$) with x of 0.01, 0.03, 0.05 and 0.07

2.2 Galvanostatic charge/discharge tests

Fig.2 shows the charge/discharge profiles for the $LiV_{1-x}Cr_xPO_4F$ cathode materials at 0.2 C rate. In this study, the charge/discharge profiles of 50 cycles are presented instead of only the first one, since lithium ion cells generally have different starting voltage during the first cycles. From Fig.2, it is clear that the initial discharge capacity of $LiVPO_4F$ is about 116.5 $mAh \cdot g^{-1}$, but the discharge capacity drops quickly to about 83.1 $mAh \cdot g^{-1}$ after 50 cycles, so the capacity loss is about 28.6% after 50 cycles. This result is in good agreement with that of Baker et al.[9,10]. However, in the Cr-doped $LiV_{1-x}Cr_xPO_4F$ system, the capacity loss was 24.1%, 4.0%, 0.9%, 3.5% for the sample with x of 0.01, 0.03, 0.05 and 0.07, respectively. Therefore, the triclinic structure becomes more tolerant to repeated charge/discharge cycles due to the Cr doping. The initial discharge capacity of $LiV_{0.99}Cr_{0.01}PO_4F$ is about 122.8 $mAh \cdot g^{-1}$, but the discharge capacity decreases quickly during the subsequent charge/discharge cycles, i.e., after 50 cycles, the discharge capacity is only 93.1 $mAh \cdot g^{-1}$. The initial capacities of $LiV_{0.97}Cr_{0.03}PO_4F$, $LiV_{0.95}B_{0.05}PO_4F$ and $LiV_{0.93}B_{0.07}PO_4F$ are 120.9, 111.0 and 110.5 $mAh \cdot g^{-1}$, respectively, and the discharge capacities are 116.0, 110.0 and 106.6 $mAh \cdot g^{-1}$, respectively after 50 cycles. Therefore, the optimal Cr doping content is that x=0.03 in order to achieve high discharge capacity and good cyclic stability in the $LiVPO_4F$ system.

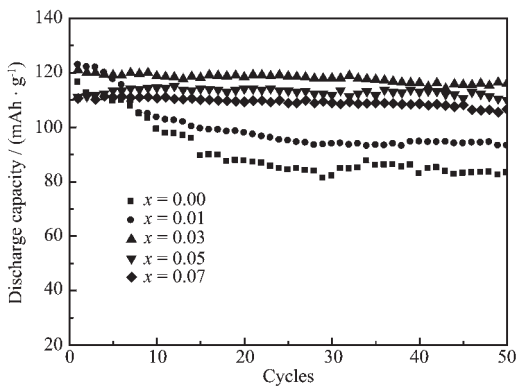

Fig.2 Discharge capacity vs cyclic number for various $LiV_{1-x}Cr_xPO_4F$ (x=0~0.07) at room temperature and 0.2 C in the voltage range of 3.0~4.6 V (vs Li^+/Li)

Fig.3 shows the first charge/discharge curves of $LiV_{0.97}Cr_{0.03}PO_4F$ sample. The sample exhibited a flat plateau around 4.3 V during charge and 4.2 V during discharge. The $LiV_{0.97}Cr_{0.03}PO_4F$ sample exhibited a higher charge capacity about 132.9 $mAh \cdot g^{-1}$ and discharge capacity about 120.9 $mAh \cdot g^{-1}$ at the current

density of 0.2 C rate. Furthermore, the sample also showed higher coulombic efficiency 91%.

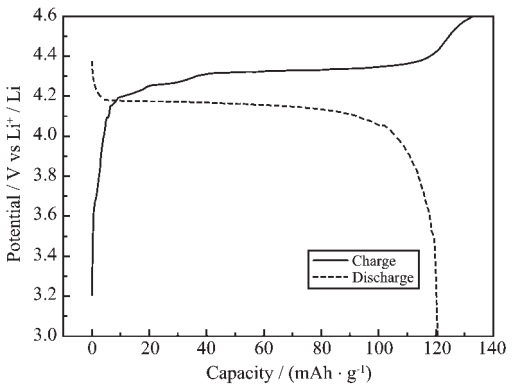

Fig.3 First charge/discharge curves of $LiV_{0.97}Cr_{0.03}PO_4F$ samples at 25 ℃ at 0.2 C rates in the voltage range of 3.0~4.6 V (vs Li^+/Li)

Galvanostatic charge/discharge tests were also conducted at different rates for $LiCr_{0.03}V_{0.97}PO_4F$ sample at room temperature in order to examine whether there is a kinetic limitation of lithium-ion transfer in the solid state, and the results are shown in Fig.4. In Fig. 4 the discharge capacity decreases at all rate with the increase of cycle number, but not sharply. After 50 cycles, the discharge capacity drops to 116.0 mAh·g^{-1} at 0.2 C rate, 101.4 mAh·g^{-1} at 0.5 C, and 97.5 mAh·g^{-1} at 1 C, respectively. Namely, the capacity decreases continuously at a rate of 0.08% per cycle at 0.2 C, 0.14% per cycle at 0.5 C, and 0.13% per cycle at 1 C.

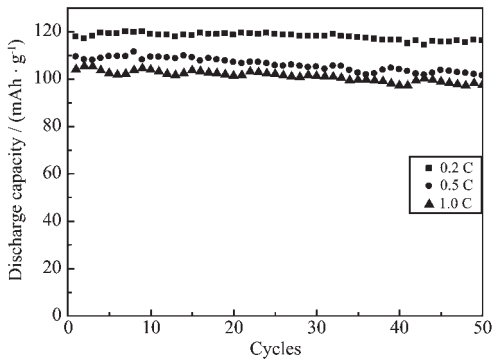

Fig.4 Cycling performance of $LiV_{0.97}Cr_{0.03}PO_4F$ samples at 25 ℃ at different rate in the voltage range of 3.0~4.6 V (vs Li^+ / Li)

The cyclic tests were performed at 25 ℃ and 55 ℃ for the $LiV_{0.97}Cr_{0.03}PO_4F$ sample between 3.0 V and 4.6 V at 0.5 C rate. The $LiV_{0.97}Cr_{0.03}PO_4F$ sample exhibited the discharge capacity of 129.2 mAh·g^{-1} at 55 ℃ for the first cycle, which is a dramatic improvement over 109.3 mAh·g^{-1} at 25 ℃. The discharge capacities at 55 ℃ were all much higher than those at 25 ℃ for all the cycles in Fig.5. The general improvement in the performance may be attributed to the increased diffusion of lithium ions at elevated temperatures.

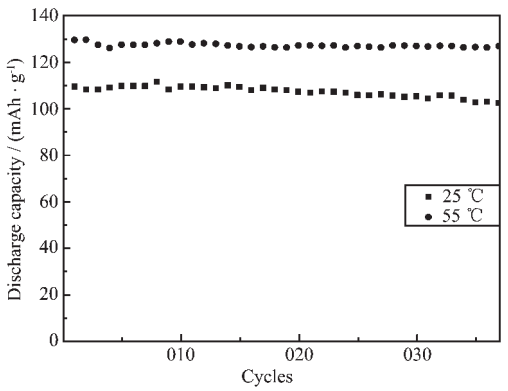

Fig.5 Cyclic performances of $LiV_{0.97}Cr_{0.03}PO_4F$ sample at 25 ℃ and 55 ℃ in the voltage range of 3.0~4.6 V (vs Li^+ / Li) at 0.5 C rate

2.3 CV measurements

CV curves for $LiVPO_4F$ and $LiV_{0.97}Cr_{0.03}PO_4F$ samples are shown in Fig.6. The curves indicate the potential in which the lithium extraction/insertion and the phase transition (if there is) occur. In the undoped system, the extraction and insertion process occurs at 4.39 V and 4.10 V, respectively. However, in the Cr-doped system, Li ion extraction potential decreases to 4.36 V,and the Li ion insertion potential increases to 4.12 V, indicating that the overpotential for both the extraction and insertion process is reduced. In CV measurements, it is known that the potential differ-

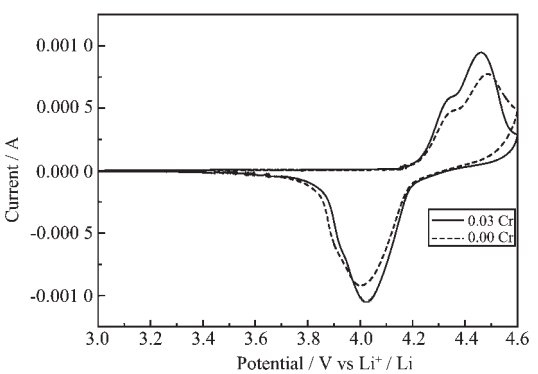

Fig.6 CV curves at scan rate of 0.1 mV·s^{-1} in the voltage range of 3.0~4.6 V for undoped $LiVPO_4F$ and $LiV_{0.97}Cr_{0.03}PO_4F$ samples

ence between anodic peak and cathodic peak is an important parameter to evaluate the reversibility of an electrochemical reaction. The potential difference of Cr-doped system is about 0.24 V, whereas that of the undoped system is about 0.29 V, showing the enhancement of electrode reaction reversibility due to the Cr-doping.

2.4 EIS analysis

The electrochemical impedance spectra of $LiVPO_4F$ and $LiV_{0.97}Cr_{0.03}PO_4F$ electrodes materials were measured at different charging states. The typical Nyquist plots of EIS are presented in Fig.7 and Fig.8 for $LiVPO_4F$ and $LiV_{0.97}Cr_{0.03}PO_4F$, respectively. A semicircle was observed to center on the real axis at the high frequency range. In the low frequency range, a straight line with an angle of 45° to the real axis corresponds to the Warburg impedance. The high-frequency semicircle is related to the charge-transfer resistance (R_{ct}) and the double-layer capacitance. The low-frequency tails resulted from the diffusion of lithium ions in the bulk active mass. Similar EIS patterns were observed for $LiVPO_4F$ and $LiV_{0.97}Cr_{0.03}PO_4F$ systems. In the case of $LiVPO_4F$, the diameter of the semicircle seemed to have significant dependence on the potential during charging, signifying that the film formation process is dependent on the lithium ion content. On the other hand, the charge transfer resistance, R_{ct}, shows a greater dependence on the lithium insertion and extraction levels. In the highly charged states, the sample was found to give lower Rct values. Comparing the diameter of the semicircle of the above two system, it can be found that $LiV_{0.97}Cr_{0.03}PO_4F$

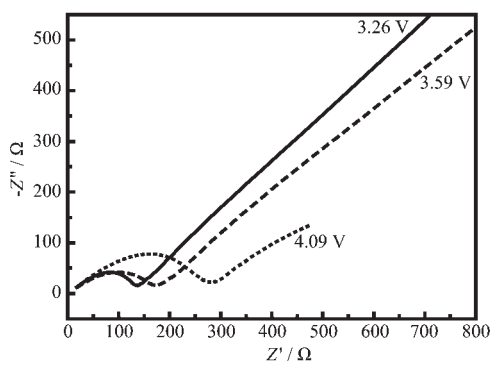

Fig.7 Nyquist plots for the EIS of $LiVPO_4F$ at different open circuit potentials

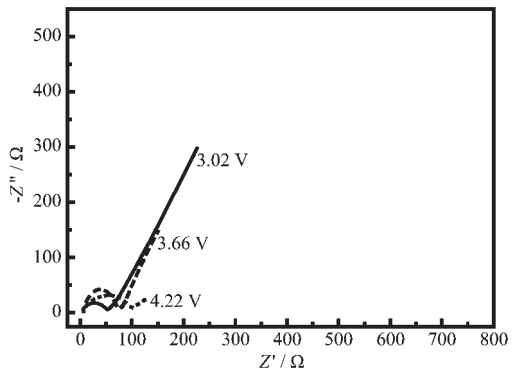

Fig.8 Nyquist plots for the EIS of $LiV_{0.97}Cr_{0.03}PO_4F$ at different open circuit potentials

showed lower R_{ct} value than $LiVPO_4F$, indicating that the Cr-doping may cause some defects in the $LiVPO_4F$ system, and increase the electronic conductivity and improve the Li^+ kinetic behavior.

The Li ion extraction/insertion processes as well as V^{3+}/V^{4+} and V^{4+}/V^{5+} redox reactions may lead to great changes to crystal structure and cause the phase instability of $LiVPO_4F$ system. Since the radius of V^{3+} is 0.074 nm, and the radius of Cr^{3+} is 0.064 nm, the existence of Cr ions would counteract the volume shrinking/swelling during the Li^+ reversible extraction/insertion, and then increase the stability of $LiVPO_4F$ phase in the long-term charge/discharge cycles. Therefore, the cyclic performances of the $LiVPO_4F$ system are apparently improved through the doping of a small amount Cr.

3 Conclusion

The Undoped and Cr-doped $LiVPO_4F$ cathode materials have been synthesized by high temperature solid-state reactions. X-ray diffraction results show that the samples are pure single triclinic phases. The Cr-doped $LiVPO_4F$ cathode materials have higher discharge capacity and better charge/discharge cyclic stability. The loss in the discharge capacity for the $LiV_{1-x}Cr_xPO_4F$ sample (x=0.01, 0.03, 0.05 and 0.07) at 0.2 C rate and room temperature is in the range of 0.9~24.1%, much lower than 28.6% of the undoped sample. The optimal doping content of Cr is that x= 0.03 to achieve high discharge capacity and good cyclic stability. In the Cr-doped system, the electrode

reaction reversibility was enhanced and the charge transfer resistance was decreased due to the Cr-doping. The Cr-doping effects can be attributed to the fact that the Cr ions with smaller size would counteract the volume shrinking/swelling during the Li^+ reversible extraction/insertion, and then increase the phase stability, resulting in the improvement of the cyclic ability. The Cr-doping may promote the application of $LiVPO_4F$ to commercial Li ion batteries.

References:

[1] Winter M, Besenhard J O, Spahr M E, et al. *Adv. Mater.*, **1998**,**10**:725~763

[2] Zhou Z, Zhao J J, Gao X P, et al. *Chem. Mater.*, **2005**,**17**: 992~1000

[3] Gao X P, Bao J L, Pan G L, et al. *J. Phys. Chem. B*, **2004**, **108**:5547~5551

[4] Pu W H, He X M, Ren J G, et al. *Electrochim. Acta*, **2005**, **50**:4140~4145

[5] Saidi M Y, Barker J, Huang H, et al. *J. Power Sources*, **2003**, **119~121**:266~272

[6] Huang H, Yin S H, Kerr T. *Adv. Mater.*, **2004**,**14**:1525~1528

[7] Dupre N, Gaubicher J, Mercier T L. *Solid State Ionics*, **2001**, **140**:209~221

[8] Richardson T J. *J. Power Sources*, **2003**,**119~121**:262~265

[9] Dutreilh M, Chevalier C, El-Ghozzi M, et al. *J. Solid State Chem.*, **1999**,**142**:1~10

[10]Barker J, Saidi M Y, Swoyer J L. *J. Electrochem. Soc.*, **2003**, **150**:1394~1398

[11]Barker J, Saidi M Y, Swoyer J L. *J. Electrochem. Soc.*, **2004**, **151**:A1670~A167

[12]Barker J, Gover R K B, Burns P, et al. *Electrochem. Solid State Lett.*, **2005**,**8**:A285~A287